

## Supporting Information

Multicolor emissive phosphorescent iridium(III) complexes containing L-alanine ligands: Photophysical and electrochemical properties, DFT calculations, and selective recognition of Cu(II) ions

Xi Chu, Yichuan Huang, Wenhao Li, Shisheng Zhao, Hongyan Li\*, Aidang Lu\*

School of Chemical Engineering and Technology, Hebei University of Technology, Tianjin 300130,

China

\* Correspondence: [hyli@hebut.edu.cn](mailto:hyli@hebut.edu.cn) (H.L.), [luaidang@hebut.edu.cn](mailto:luaidang@hebut.edu.cn) (A.L.)

## Table of Contents

**Figure S1.** The  $^1\text{H}$  NMR spectrum of the complex **Ir1**.

**Figure S2.** The  $^{13}\text{C}$  NMR spectrum of the complex **Ir1**.

**Figure S3.** The  $^1\text{H}$  NMR spectrum of the complex **Ir2**.

**Figure S4.** The  $^{13}\text{C}$  NMR spectrum of the complex **Ir2**.

**Figure S5.** The  $^1\text{H}$  NMR spectrum of the complex **Ir3**.

**Figure S6.** The  $^{13}\text{C}$  NMR spectrum of the complex **Ir3**.

**Figure S7.** The  $^{19}\text{F}$  NMR spectrum of the complex **Ir2**.

**Figure S8.** The  $^{19}\text{F}$  NMR spectrum of the complex **Ir3**.

**Figure S9.** Photoluminescence spectra of **Ir1** upon addition of various metal ions (10 equiv.) in acetonitrile solutions.

**Figure S10.** Photoluminescence spectra of **Ir2** upon addition of various metal ions (10 equiv.) in acetonitrile solutions.

**Figure S11.** Photoluminescence spectra of **Ir3** upon addition of various metal ions (10 equiv.) in acetonitrile solutions.

**Figure S12.** The emission spectra of **Ir1–Ir3** in the absence of  $\text{Cu}^{2+}$  (black line), in the presence of  $\text{Cu}^{2+}$  (red line) and in presence of both  $\text{Cu}^{2+}$  and  $\text{Na}_2\text{EDTA}$  (blue line) in  $\text{CH}_3\text{CN}$ . (a) **Ir1** (b) **Ir2** (c) **Ir3**

**Figure S13.**  $^1\text{H}$  NMR ( $\text{DMSO}-d_6$ ) spectra of complex **Ir2** (red line) and **Ir2** + 1.0 equiv. of  $\text{Cu}^{2+}$  (green line).

**Scheme S1.** Possible sensing mechanism of **Ir2** with  $\text{Cu}^{2+}$ .

**Table S1.** Distribution of energy and electron density along the orbit of frontier molecules of **Ir1**.

**Table S2.** Distribution of energy and electron density along the orbit of frontier molecules of **Ir2**.

**Table S3.** Distribution of energy and electron density along the orbit of frontier molecules of **Ir3**.

**Table S4.** Summary of the results of TD-DFT calculations on complex **Ir1** (assignment is provided for MO contributions  $> 10\%$ )

**Table S5.** Summary of the results of TD-DFT calculations on complex **Ir2**

(assignment is provided for MO contributions > 10 %)

**Table S6.** Summary of the results of TD-DFT calculations on complex **Ir3**

(assignment is provided for MO contributions > 10 %)

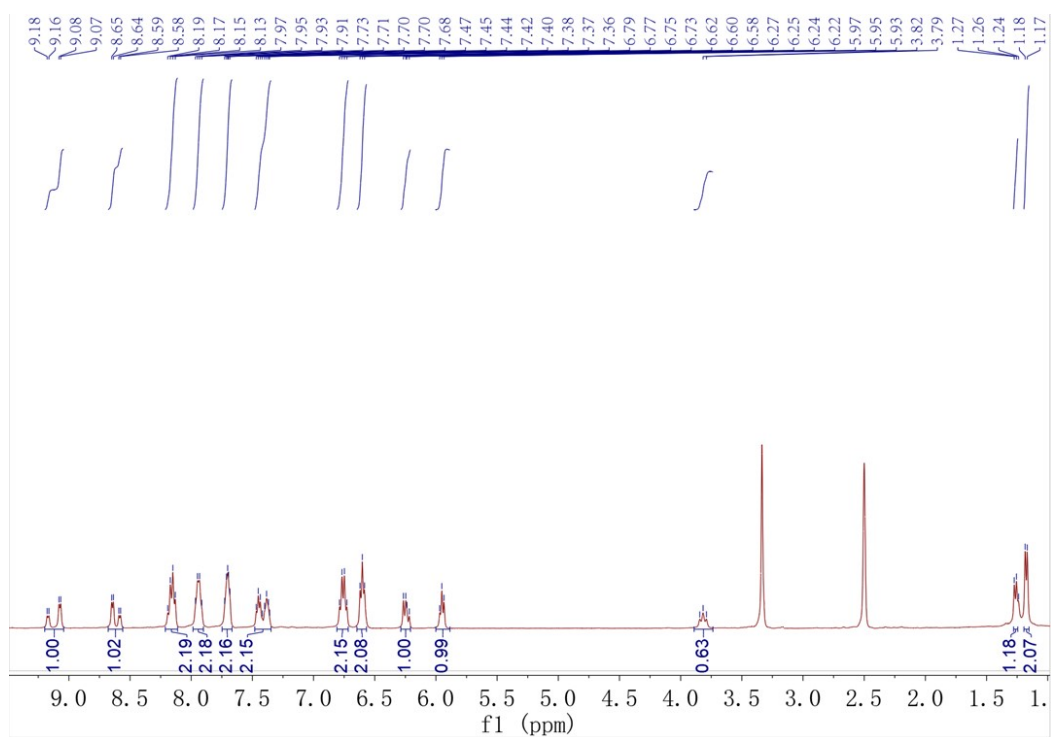


**Figure S1.** The <sup>1</sup>H NMR spectrum of the complex **Ir1**.

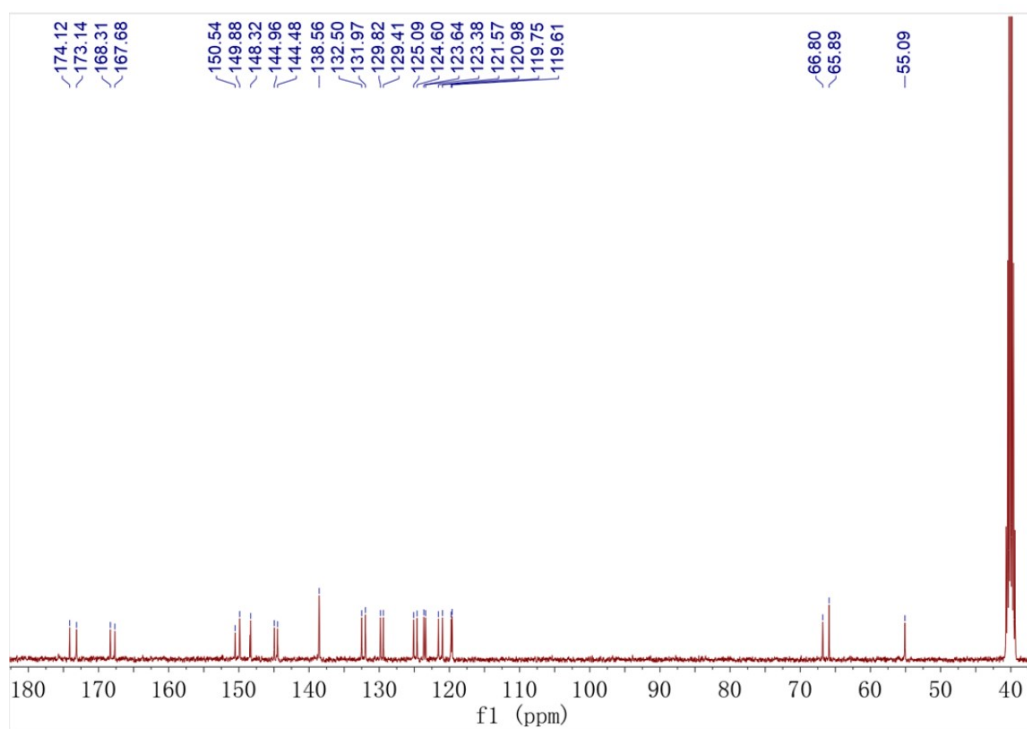


**Figure S2.** The <sup>13</sup>C NMR spectrum of the complex **Ir1**.

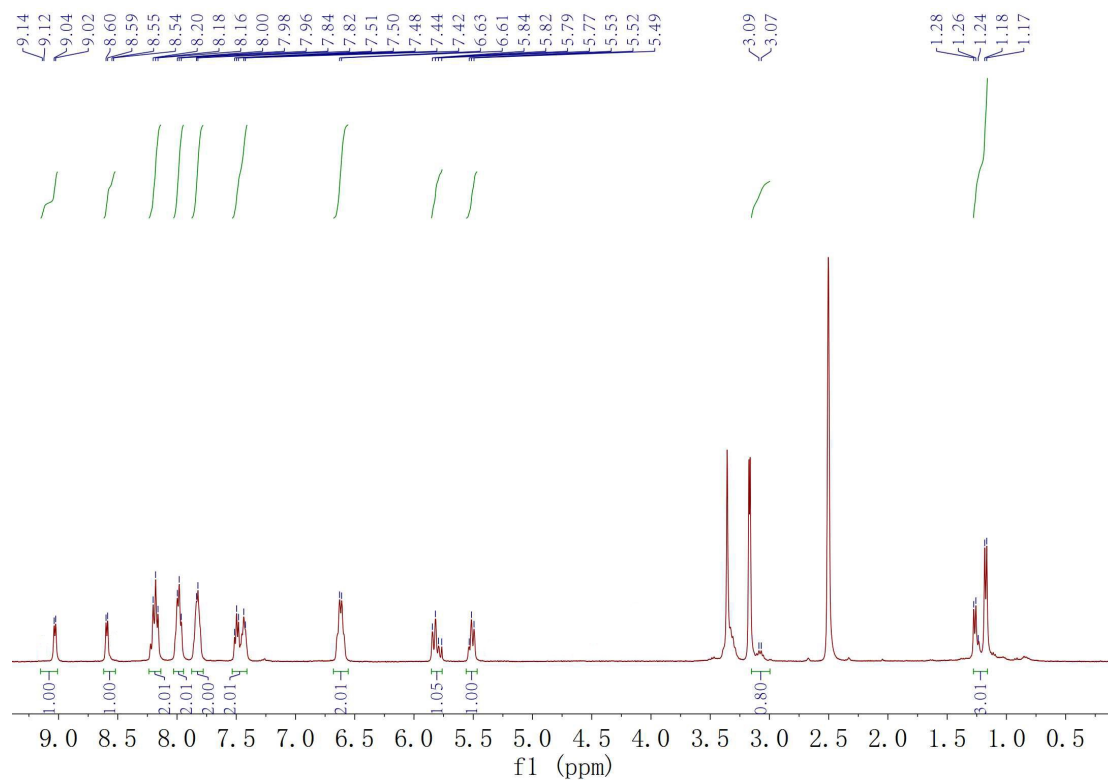


**Figure S3.** The <sup>1</sup>H NMR spectrum of the complex **Ir2**.

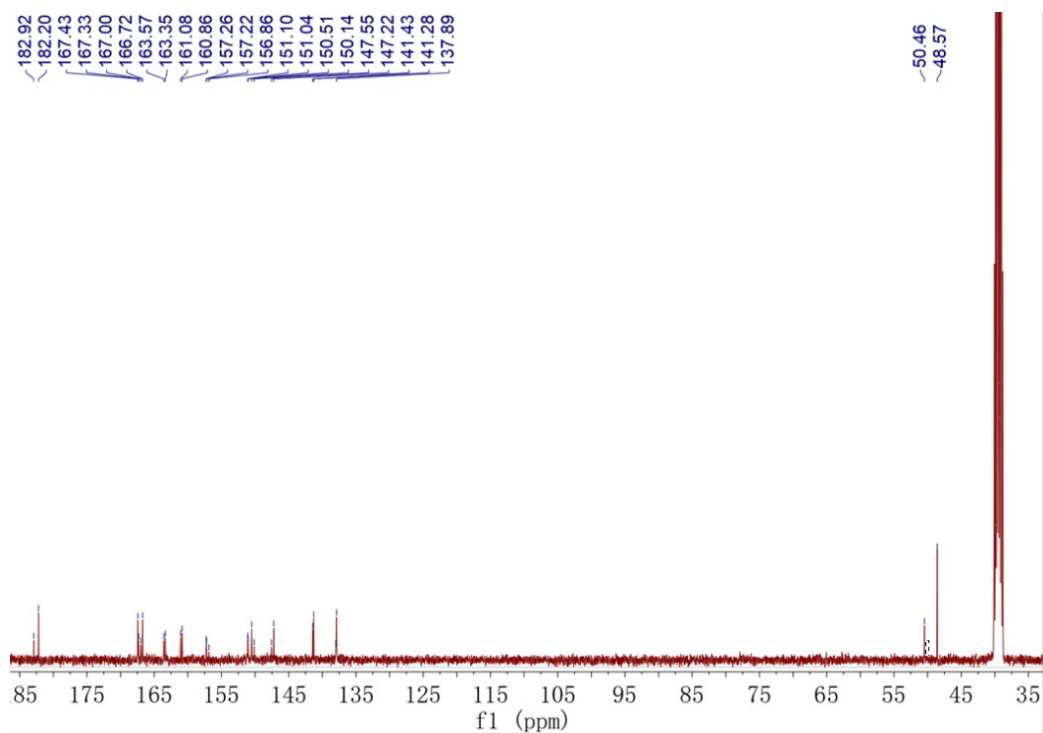


**Figure S4.** The <sup>13</sup>C NMR spectra of the complex **Ir2**.

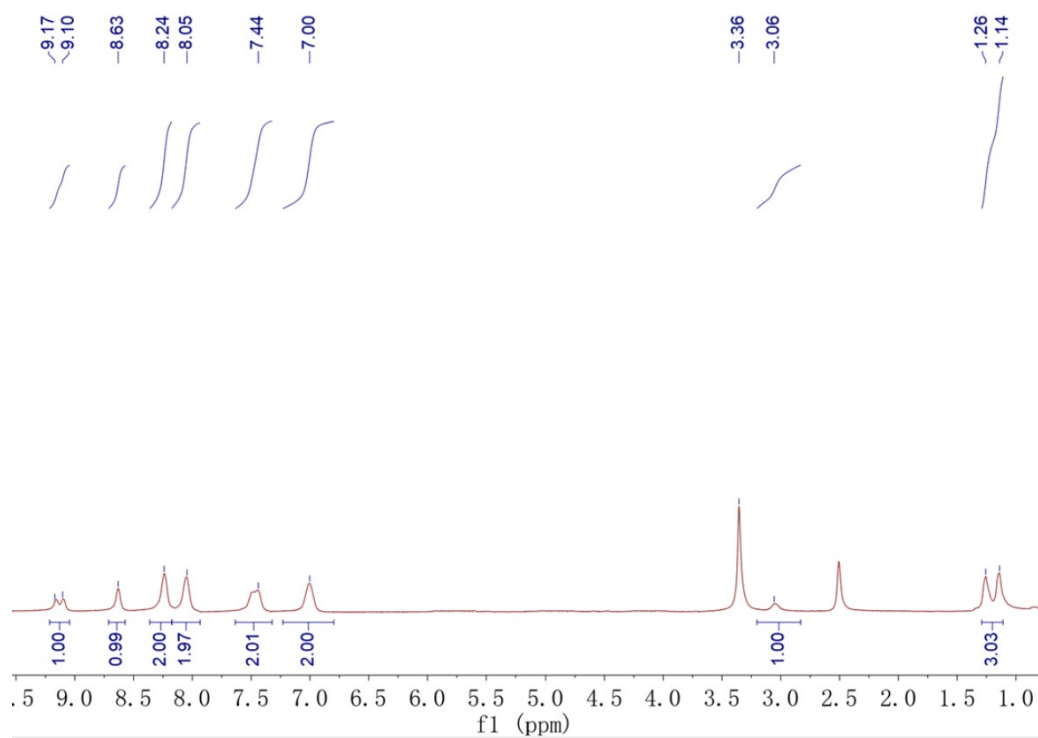


**Figure S5.** The <sup>1</sup>H NMR spectrum of the complex **Ir3**.

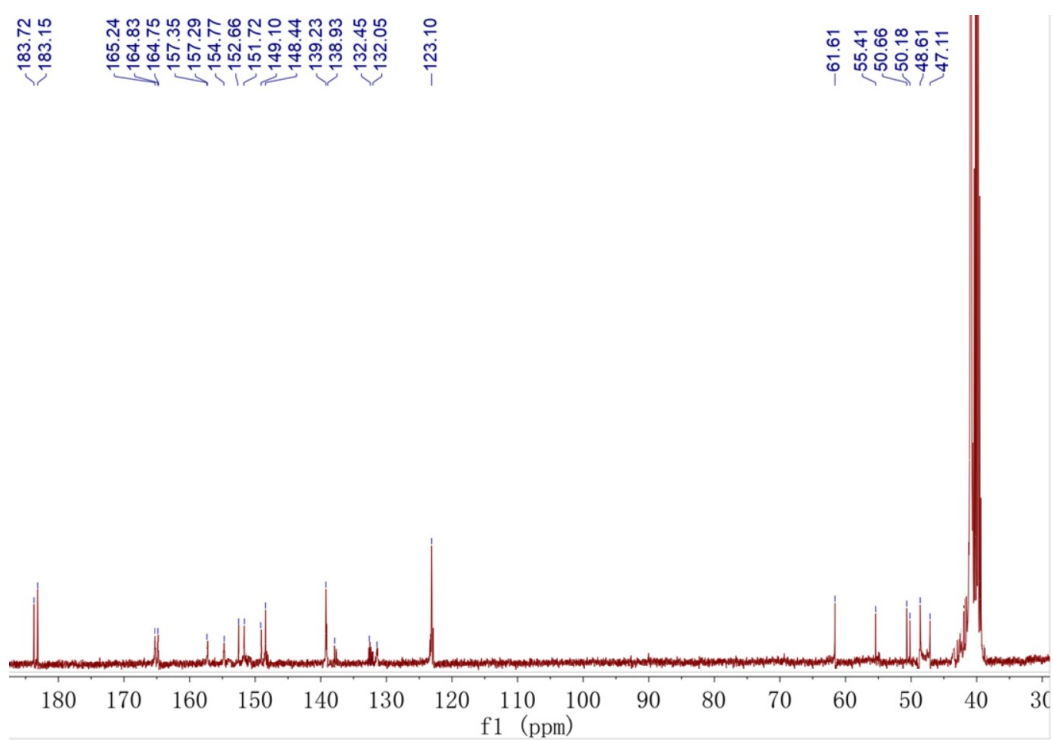


**Figure S6.** The <sup>13</sup>C NMR spectrum of the complex **Ir3**.

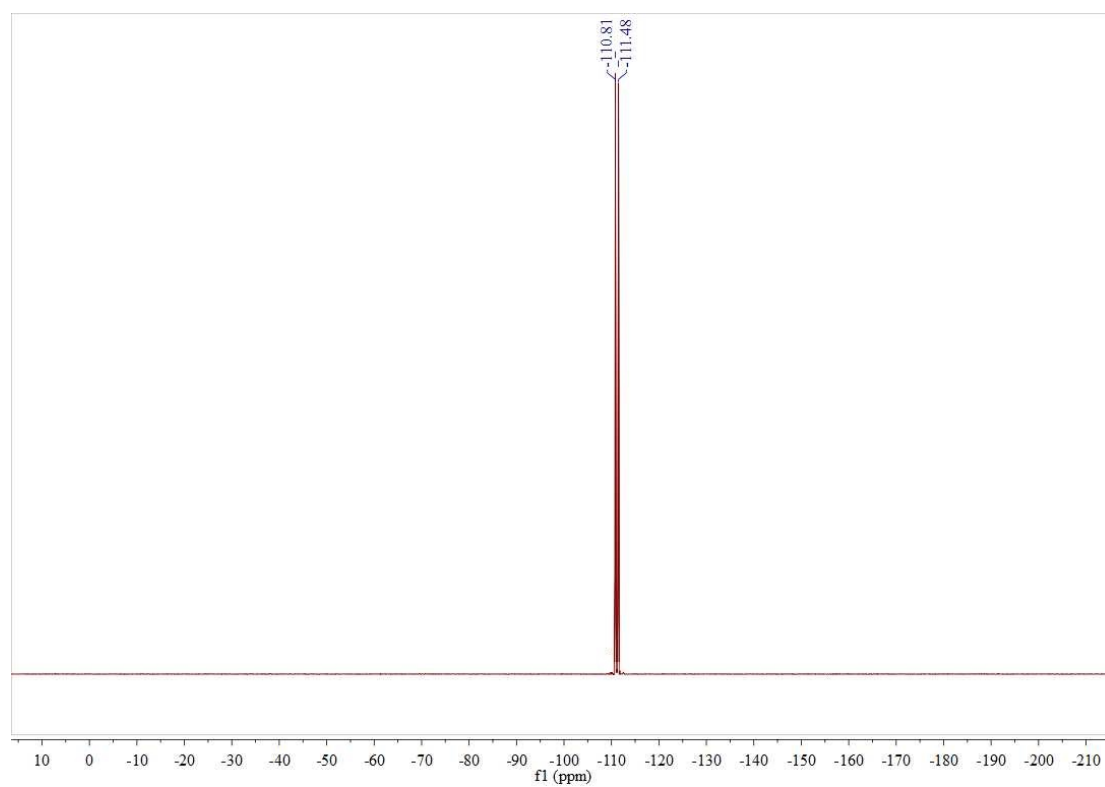


**Figure S7.** The  $^{19}\text{F}$  NMR spectrum of the complex **Ir2**.

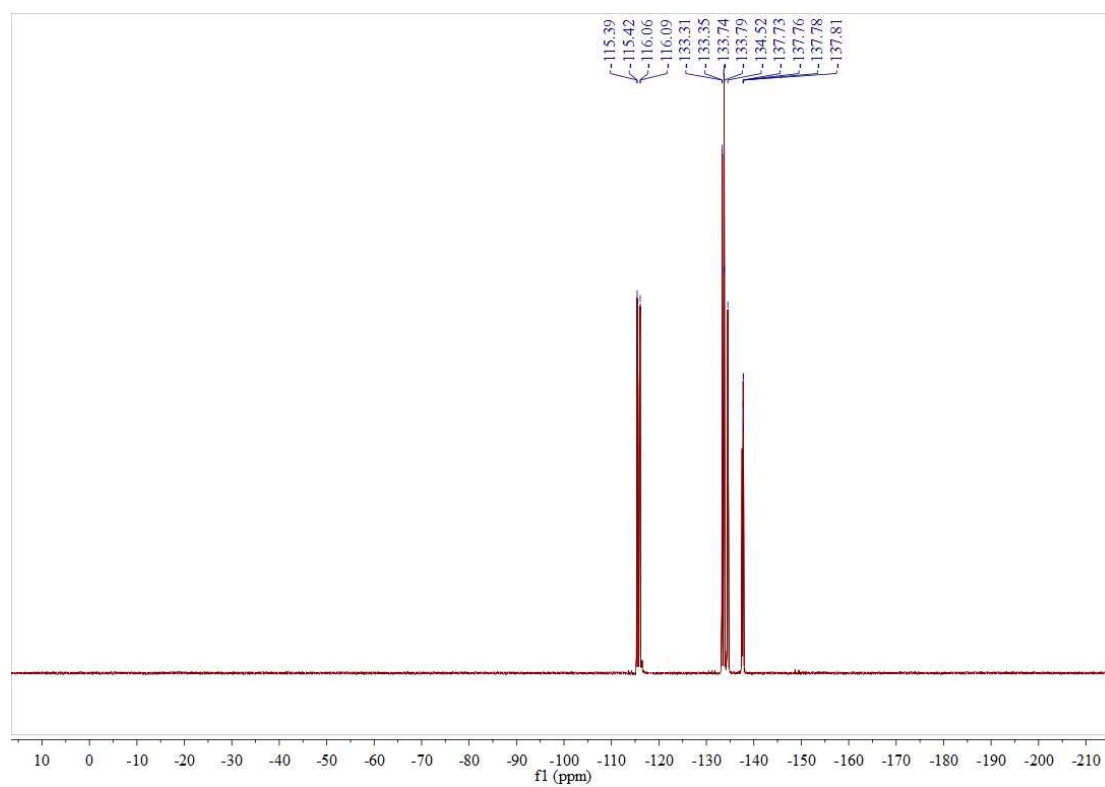


**Figure S8.** The  $^{19}\text{F}$  NMR spectrum of the complex **Ir3**.

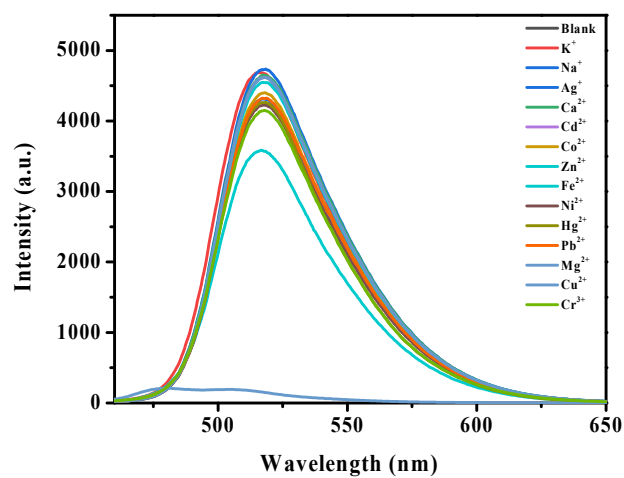


**Figure S9.** Photoluminescence spectra of **Ir1** upon addition of various metal ions (10.0 equiv.) in acetonitrile solutions.

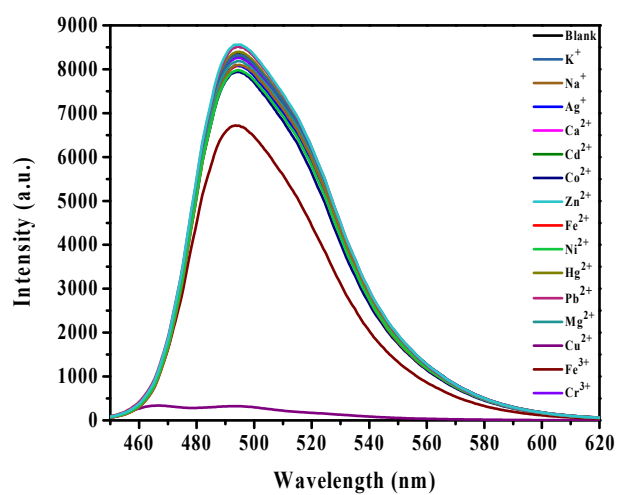


**Figure S10.** Photoluminescence spectra of **Ir2** upon addition of various metal ions (10.0 equiv.) in acetonitrile solutions.



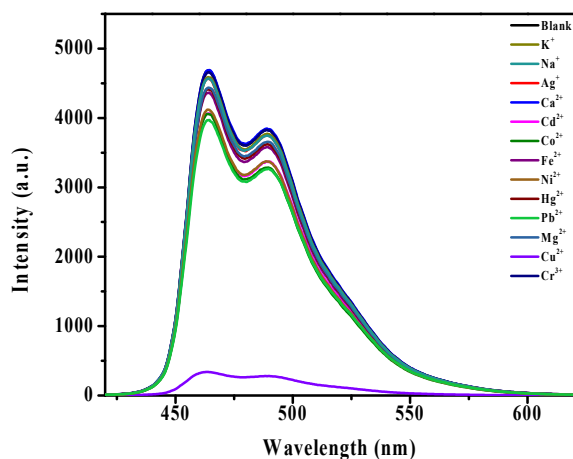


**Figure S11.** Photoluminescence spectra of **Ir3** upon addition of various metal ions (10.0 equiv.) in acetonitrile solutions.

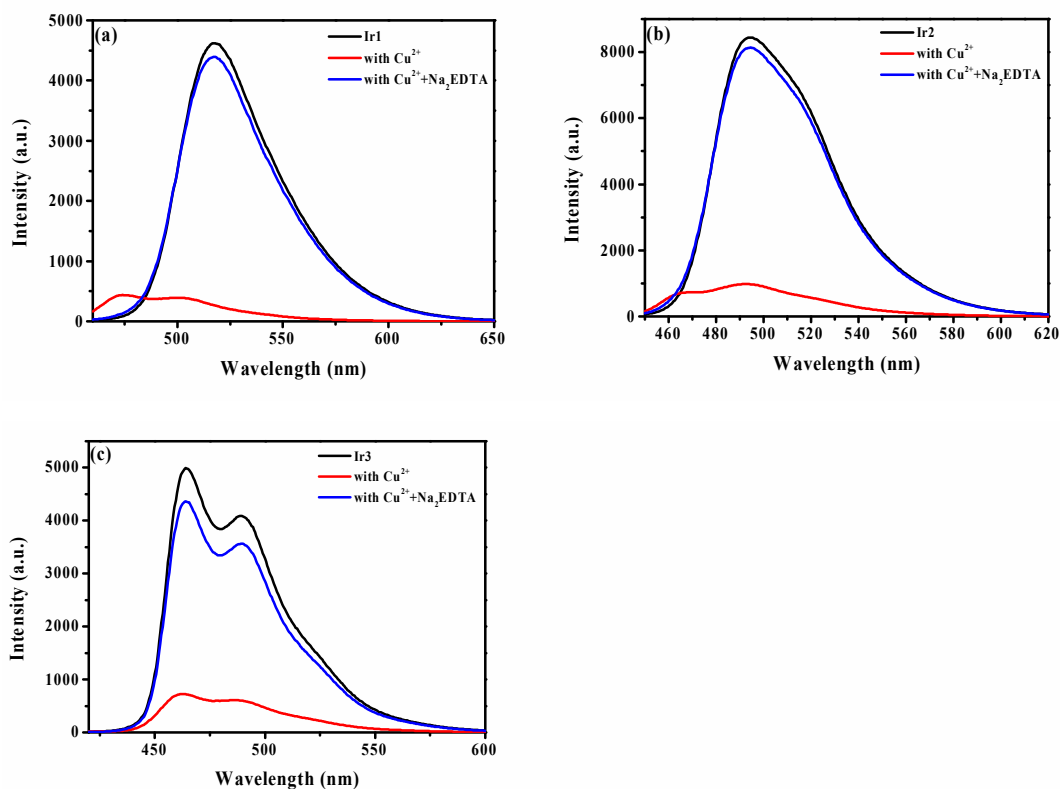


**Figure S12.** The emission spectra of **Ir1–Ir3** in the absence of  $\text{Cu}^{2+}$  (black line), in the presence of  $\text{Cu}^{2+}$  (red line) and in the presence of both  $\text{Cu}^{2+}$  and  $\text{Na}_2\text{EDTA}$  (blue line) in  $\text{CH}_3\text{CN}$  solution. (a) **Ir1** (b) **Ir2** (c) **Ir3**.

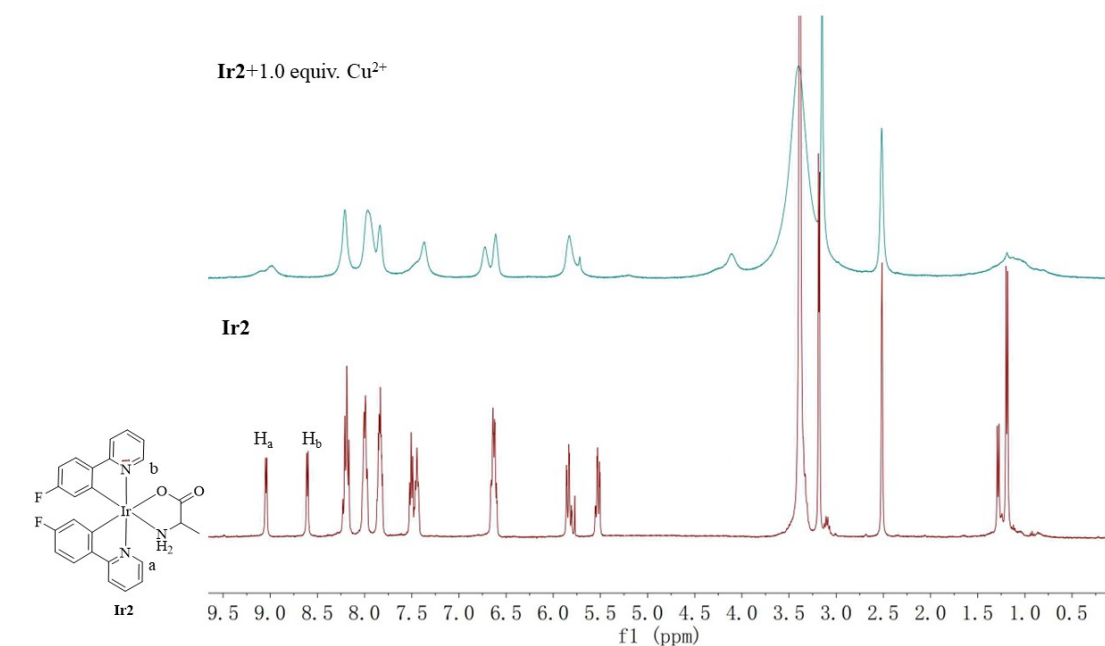
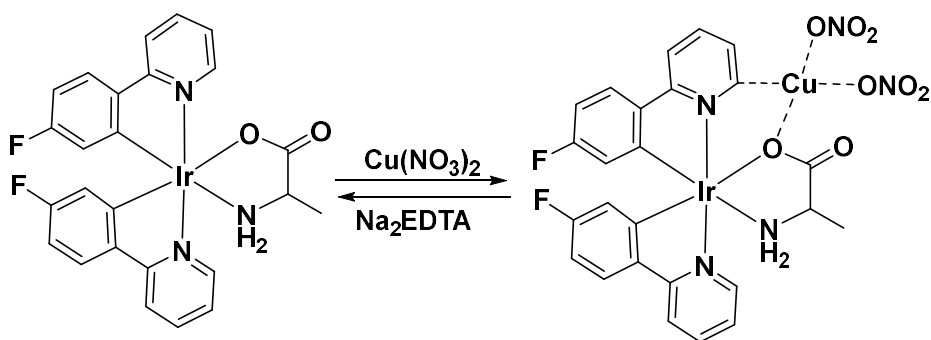


**Figure S13.**  $^1\text{H}$  NMR (DMSO- $d_6$ ) spectra of complex **Ir2** (red line) and **Ir2** + 1.0 equiv. of  $\text{Cu}^{2+}$  (green line).



**Scheme S1.** Possible sensing mechanism of **Ir2** with  $\text{Cu}^{2+}$ .

**Table S1.** Distribution of energy and electron density along the orbit of frontier molecules of **Ir1**.

Complex	Orbital	Energy (eV) (Calculated)	Composition %			
			Ir	Cyclometalated ligands		Ancillary ligands
				phenyl	pyridyl	
<b>Ir1</b>	HOMO-5	-6.439	6.10	20.88	6.65	66.38
	HOMO-4	-6.415	16.07	56.30	24.25	3.38
	HOMO-3	-6.213	57.19	23.92	12.70	6.18
	HOMO-2	-6.135	18.55	50.19	23.41	7.85
	HOMO-1	-5.869	63.52	9.20	11.13	16.15
	HOMO	-5.217	52.28	35.88	6.24	5.60
	LUMO	-1.571	4.79	26.68	66.42	2.12
	LUMO+1	-1.519	5.05	22.43	70.27	2.25
	LUMO+2	-1.047	3.23	12.91	80.99	2.86
	LUMO+3	-0.943	3.31	10.94	83.72	2.03
	LUMO+4	-0.153	10.92	72.99	5.33	10.77

**Table S2.** Distribution of energy and electron density along the orbit of frontier molecules of **Ir2**.

Complex	Orbital	Energy (eV) (Calculated)	Composition %			
			Ir	Cyclometalated ligands		Ancillary ligands
				phenyl	pyridyl	
<b>Ir2</b>	HOMO-5	-6.491	4.01	16.11	2.52	77.36
	HOMO-4	-6.427	49.07	31.57	16.05	3.30
	HOMO-3	-6.309	41.09	34.93	16.46	7.52
	HOMO-2	-6.144	16.42	52.27	23.72	7.59
	HOMO-1	-5.954	57.88	13.80	12.77	15.55
	HOMO	-5.372	50.50	36.23	7.57	5.71
	LUMO	-1.581	4.76	25.91	67.20	2.13
	LUMO+1	-1.534	4.83	22.07	70.91	2.19
	LUMO+2	-1.084	3.16	15.56	78.45	2.83
	LUMO+3	-0.973	3.33	12.04	82.63	2.00
	LUMO+4	-0.061	8.08	76.69	6.86	8.36

**Table S3.** Distribution of energy and electron density along the orbit of frontier molecules of **Ir3**.

Complex	Orbital	Energy (eV) (Calculated)	Composition %			
			Ir	Cyclometalated ligands		Ancillary ligands
				phenyl	pyridyl	
<b>Ir3</b>	HOMO-5	-6.655	34.72	8.19	9.56	48.74
	HOMO-4	-6.547	21.67	37.90	10.22	31.05
	HOMO-3	-6.392	17.62	50.60	21.91	10.01
	HOMO-2	-6.294	10.59	67.16	21.46	0.82
	HOMO-1	-6.144	48.87	24.21	11.95	15.20
	HOMO	-5.641	50.82	38.30	4.62	6.57
	LUMO	-1.686	4.49	26.85	66.01	2.68
	LUMO+1	-1.682	5.05	27.71	65.26	2.08
	LUMO+2	-1.032	1.96	10.56	84.08	3.61
	LUMO+3	-1.014	3.23	10.98	84.12	1.79
	LUMO+4	-0.182	17.49	66.71	5.16	10.92

**Table S4.** Summary of the results of TD-DFT calculations on complex **Ir1**  
(assignment is provided for MO contributions > 10 %)

No.	Energy (cm <sup>-1</sup> )	Wavelength (nm)	<i>f</i>	MOs1	MOs2	MOs3	MOs4
1	23266	430	0.0639	HOMO→LUMO (97 %)			
2	28060	356	0.0135	HOMO→L+2 (97 %)			
3	28784	347	0.0356	HOMO→L+3 (55 %)	H-1→L+1 (31 %)	H-1→LUMO (11 %)	
4	29162	343	0.0543	HOMO→L+3 (42 %)	H-1→L+1 (32 %)	H-1→LUMO (20 %)	
5	31433	318	0.0621	H-3→L+1 (27 %)	H-2→L+1 (26 %)	H-2→LUMO (24 %)	H-3→LUMO (12 %)
6	32058	312	0.0144	H-2→LUMO (40 %)	H-3→LUMO (-24 %)	H-1→L+2 (20 %)	
7	32531	307	0.0804	H-2→L+1 (38 %)	H-3→L+1 (35 %)	H-3→LUMO (11 %)	
8	33130	302	0.0164	H-1→L+2 (66 %)			
9	33629	297	0.0225	H-1→L+3 (67 %)	H-4→LUMO (16 %)		
10	34344	291	0.061	H-2→L+2 (11 %)	H-4→LUMO (25 %)	H-5→LUMO (15 %),	
11	34889	287	0.0382	H-5→L+1 (48 %)	H-4→LUMO (29 %)		
12	35223	284	0.166	H-5→L+1 (30 %)	H-4→L+1 (20 %)	H-1→L+3 (11 %)	HOMO→L+4 (10 %)
13	36453	274	0.0832	HOMO→L+4 (40 %)	H-2→L+3 (14 %),	H-3→L+2 (12 %)	
14	36881	271	0.0767	H-2→L+2 (39 %)	H-3→L+2 (20 %),	HOMO→L+4 (11 %)	
15	37317	268	0.1275	H-3→L+3 (59 %)			
16	37776	265	0.3217	H-2→L+3 (57 %)			
17	38064	263	0.0209	HOMO→L+9 (32 %)	HOMO→L+5 (16 %)	HOMO→L+7 (17 %)	
18	39019	256	0.0313	H-4→L+2 (44 %)			
19	39056	256	0.0106	H-5→L+2 (75 %)	H-4→L+2 (13 %)		
20	39306	254	0.0129	H-7→L+1 (72 %)			

**Table S5.** Summary of the results of TD-DFT calculations on complex **Ir2**  
(assignment is provided for MO contributions > 10 %)

No.	Energy (cm <sup>-1</sup> )	Wavelength (nm)	<i>f</i>	MOs1	MOs2	MOs3	MOs4
1	24406	410	0.0632	HOMO→LUMO (97 %)			
2	29049	344	0.0138	HOMO→L+2 (95 %)			
3	29560	338	0.0691	H-1→L+1 (52 %)	H-1→LUMO (25 %)	HOMO→L+3 (15 %)	
4	30059	333	0.0150	HOMO→L+3 (82 %)			
5	31215	320	0.0129	H-3→LUMO (26 %)	H-2→LUMO (23 %)	H-4→LUMO (16 %)	H-3→L+1 (13 %)
6	31979	313	0.0563	H-2→L+1 (35 %)	H-2→LUMO (31 %)	H-3→L+1 (12 %)	H-4→L+1 (10 %)
7	32391	309	0.0349	H-2→LUMO (25 %)	H-3→LUMO (22 %)	H-2→L+1 (16 %)	
8	32994	303	0.0944	H-3→L+1 (31 %),	H-2→L+1 (22 %)	H-3→LUMO (16 %)	H-4→L+1 (14 %),
9	33899	295	0.0256	H-4→LUMO (39 %)	H-1→L+3 (35 %)	H-3→LUMO (15 %)	
10	34342	291	0.0535	H-4→L+1 (35 %)	H-3→L+1 (17 %)	H-1→L+3 (16 %)	
11	34830	287	0.0641	H-5→LUMO (37 %)	H-1→L+3 (14 %)	H-3→L+1 (10 %)	
12	35150	284	0.1061	H-5→LUMO (49 %)	H-5→L+1 (-12 %)		
13	35355	283	0.0604	H-5→L+1 (71 %)			
14	36056	277	0.0409	H-2→L+2 (43 %)	H-3→L+2 (12 %)	H-6→LUMO (10 %)	
15	36417	275	0.1176	HOMO→L+4 (56 %)	H-3→L+2 (11 %),		
16	36924	271	0.1000	H-6→L+1 (46 %)	H-2→L+3 (14 %)	H-3→L+2 (15 %)	
17	37844	264	0.1389	H-3→L+3 (42 %)	H-4→L+3 (19 %)		
18	37944	264	0.1769	H-2→L+3 (43 %)	H-6→L+1 (18 %)	H-3→L+3 (13 %)	
19	38287	261	0.0192	HOMO→L+7 (27 %)	H-1→L+7 (11 %)	H-3→L+2 (10 %)	
20	38583	259	0.0887	H-4→L+2 (52 %)	H-3→L+2 (17 %)		

**Table S6.** Summary of the results of TD-DFT calculations on complex **Ir3**  
(assignment is provided for MO contributions > 10 %)

No.	Energy (cm <sup>-1</sup> )	Wavelength (nm)	<i>f</i>	MOs1	MOs2	MOs3	MOs4
1	25583	391	0.0536	HOMO→L+1 (84 %)	HOMO→LUMO (14 %)		
2	30227	331	0.0842	H-1→L+1 (77 %)	H-1→LUMO (11 %)		
3	31566	317	0.0172	HOMO→L+2 (91 %)			
4	32441	308	0.1099	H-2→LUMO (57 %)	H-2→L+1 (15 %)		
5	33183	301	0.1304	H-3→L+1 (53 %)	H-1→L+2 (13 %)	H-3→LUMO (10 %)	
6	33348	300	0.0149	H-3→LUMO (59 %)	H-3→L+1 (13 %)		
7	33882	295	0.0363	H-4→LUMO (26 %)	H-4→L+1 (23 %)	H-2→L+1 (14 %)	
8	34015	294	0.1036	H-4→LUMO (26 %)	H-4→L+1 (24 %)	H-3→LUMO (11 %)	
9	34809	287	0.0147	H-5→LUMO (29 %)	H-6→LUMO (16 %)	H-4→LUMO (14 %)	H-4→L+1 (10 %)
10	35783	279	0.0470	H-1→L+2 (35 %)	HOMO→L+4 (21 %)	H-6→L+1 (10 %)	
11	36020	278	0.0136	H-6→L+1 (43 %),	HOMO→L+4 (18 %)	H-5→L+1 (16 %)	
12	36479	274	0.1804	H-1→L+2 (29 %)	HOMO→L+4 (14 %)	HOMO→L+6 (11 %)	H-6→L+1 (11 %)
13	37357	268	0.0105	HOMO→L+7 (30 %)	HOMO→L+5 (24 %)		
14	37760	265	0.0348	H-2→L+2 (57 %)			
15	38037	263	0.0100	HOMO→L+5 (-16 %)	HOMO→L+7 (16 %)	H-1→L+7 (13 %)	H-2→L+2 (-10 %)
16	38297	261	0.2198	H-2→L+3 (65 %)			
17	38716	258	0.0364	H-3→L+2 (65 %)			
18	39817	251	0.0240	H-4→L+3 (64 %)			